Influence of Thermal Stratification on Seasonal Net Ecosystem Production and Dissolved Inorganic Carbon in a Shallow Subtropical Lake

Lin, Hao-Chi ; Chiu, Chih-Yu ; Tsai, Jeng-Wei ; Liu, Wen-Cheng ; Tada, Kazufumi ; Nakayama, Keisuke

(Citation)
JGR: Biogeosciences,126(4):e2020JG005907

(Issue Date)
2021-04

(Resource Type)
journal article

(Version)
Version of Record

JGR Biogeosciences

RESEARCH ARTICLE
10.1029/2020JG005907

Special Section:
Water-energy-carbon fluxes over terrestrial water surfaces

Influence of Thermal Stratification on Seasonal Net Ecosystem Production and Dissolved Inorganic Carbon in a Shallow Subtropical Lake

Hao-Chi Lin[1], Chih-Yu Chiu[2], Jeng-Wei Tsai[3], Wen-Cheng Liu[4], Kazufumi Tada[5], and Keisuke Nakayama[1]

[1]Graduate School of Engineering, Kobe University, Kobe City, Japan, [2]Biodiversity Research Center, Academia Sinica, Taipei, Taiwan, [3]Department of Biological Science and Technology, China Medical University, Taichung City, Taiwan, [4]Department of Civil and Disaster Prevention Engineering, National United University, Miao-Li, Taiwan, [5]Chuden Engineering Consultants, Hiroshima, Japan

Key Points:

- Typhoons play a major role in the carbon (C) release in a shallow lake
- A model is presented to evaluate net ecosystem production using the residence time of a lake
- Estimates of dissolved inorganic C demonstrate the importance of simulating stratification in a lake

Correspondence to:
K. Nakayama,
nakayama@phoenix.kobe-u.ac.jp

Citation:
Lin, H.-C., Chiu, C.-Y., Tsai, J.-W., Liu, W.-C., Tada, K., & Nakayama, K. (2021). Influence of thermal stratification on seasonal net ecosystem production and dissolved inorganic carbon in a shallow subtropical lake. *Journal of Geophysical Research: Biogeosciences*, *126*, e2020JG005907. https://doi.org/10.1029/2020JG005907

Received 14 JUN 2020
Accepted 24 JAN 2021

Author Contributions:
Conceptualization: Hao-Chi Lin
Formal analysis: Hao-Chi Lin
Funding acquisition: Chih-Yu Chiu, Wen-Cheng Liu
Investigation: Hao-Chi Lin, Jeng-Wei Tsai
Methodology: Kazufumi Tada, Keisuke Nakayama
Project Administration: Chih-Yu Chiu, Wen-Cheng Liu
Resources: Wen-Cheng Liu
Software: Kazufumi Tada, Keisuke Nakayama
Supervision: Keisuke Nakayama
Writing – original draft: Hao-Chi Lin
Writing – review & editing: Chih-Yu Chiu, Jeng-Wei Tsai, Wen-Cheng Liu, Kazufumi Tada, Keisuke Nakayama

Abstract Thermal stratification is a critical physical process controlling carbon (C) flux from lakes into the atmosphere. In general, vertical water temperature profiles in shallow subtropical lakes can vary significantly because typhoons frequently induce vertical mixing across the entire lake due to strong winds and rapid flushing from river inputs. Since C fluxes are driven by dissolved inorganic C (DIC), it is necessary to understand stratification's influence on DIC dynamics in shallow subtropical lakes. Therefore, we aimed to clarify the impact of stratification on DIC in Yuan-Yang Lake, a typical shallow subtropical mountain lake, by developing a net ecosystem production (NEP) model. We measured the vertical profile of water temperature and DIC once or twice a month from July 2004 to December 2017. We applied a three-dimensional hydrological model to estimate residence time and NEP, which revealed that large amounts of DIC are stored in the lower layer from spring to summer due to the suppression of vertical mixing by stratification. In autumn and winter, the lake was well mixed, and DIC was evenly distributed in the water column due to vertical mixing. This was confirmed by vertical DIC profiles.

Plain Language Summary Vertical distribution of dissolved inorganic C (DIC) is one of the most important factors for understanding C emission from lakes. Thermal stratification is expected to be the critical physical process controlling the vertical distribution of DIC. To clarify the relationship between DIC and thermal stratification, we investigated vertical profiles of DIC and the strength of stratification in a subtropical shallow lake (Yuan-Yang Lake [YYL]) using field observations from 2004 to 2017. Our study is the first to apply a three-dimensional hydrological model to clarify the mechanism controlling the vertical profile of DIC as part of an estimate of net ecosystem production in a lake.

1. Introduction

Freshwater ecosystems release substantial amounts of carbon (C) into the atmosphere: approximately 0.3–1.8 Pg C yr^{-1} (Aufdenkampe et al., 2011; Engel et al., 2018; Lauerwald et al., 2015; Raymond et al., 2013). Small lakes (lake area < 0.1 km^2) occupy 25%–35% of the total area of all lakes in the world (Downing et al., 2006; Verpoorter et al., 2014). However, C emissions from small lakes are usually ignored when evaluating C fluxes (Cole et al., 2007; Raymond et al., 2013), resulting in an underestimation of CO_2 emissions on a global scale (Downing et al., 2006; Verpoorter et al., 2014). Lake size has also been revealed to be one of the most critical factors controlling CO_2 emissions, with small lakes having more considerable contributions from convection to gas transfer velocities (Read et al., 2012; Vachon & del Giorgio, 2014). Heavy rainfall, wind shear, and convective mixing are essential meteorological forces that cause vertical mixing in small lakes; in shallow lakes, stratification can cause internal waves, which in turn can cause mass transport (Kimura et al., 2012, 2014, 2017). Therefore, to accurately estimate C fluxes from small lakes, it is necessary to clarify the mechanisms of vertical mixing and the collapse of stratification.

There are many mountainous shallow lakes in subtropical East Asia. For example, in Taiwan, previous studies have shown that seasonal and annual C fluxes are frequently influenced by typhoon and monsoon events, but C fluxes from subtropical lakes above an altitude of 1,500 m are not well understood (Jones et al., 2009; Tsai et al., 2008, 2011,2016). The typhoon season is from July to October, and typhoons contribute to 10%–

37% of the island's annual precipitation (Chiu et al., 2020; Lai et al., 2006; Tsai et al., 2011). Typhoon-induced rapid flushing can mix the entire water body in a small subtropical lake, likely eliminating thermal stratification (Kimura et al, 2012, 2014; Shade et al., 2010; Tsai et al., 2008). It has also been demonstrated that strong typhoon disturbances alter water levels, water quality, lake metabolism, and CO_2 fluxes in shallow subtropical lakes (Chiu et al., 2020; Jones et al., 2009; Tsai et al., 2008, 2011,2016). Jones et al. (2009) showed that the frequency of typhoons had the most significant impact on CO_2 fluxes in a shallow subtropical lake, increasing fluxes by approximately 2,200 kg C yr^{-1} per typhoon event. On the other hand, an absence of precipitation may affect CO_2 dynamics across the air-water interface in subtropical lakes (Chiu et al., 2020; Xu & Xu, 2018). Long-term investigations of shallow subtropical lakes, such as those at seasonal and annual scales, are rare but valuable. Further research on small shallow lakes in subtropical regions is necessary to clarify their physical structure and estimate C fluxes accurately.

CO_2 concentrations can be estimated from water temperature, salinity, dissolved inorganic C (DIC), and pH or total alkalinity (TA) (Cai & Wang, 1998; Smith, 1985). If we ignore calcification, DIC is principally associated with the partial pressure of CO_2 (pCO_2) (Bade et al., 2004; Striegl et al., 2001). Previous studies showed that C fluxes in boreal lakes were mainly derived by DIC inputs (McDonald et al., 2013; Weyhenmeyer et al., 2015). In general, DIC concentrations in the epilimnion are lower than in the hypolimnion of stratified lakes because photosynthesis dramatically decreases pCO_2 in the epilimnion during the day (Gruber et al., 2000). In addition, mineralization of dissolved organic C (Kortelainen et al., 2006) and carbonate deposition (or dissolution) in sediments at the lake bottom (Einsele et al., 2001) are associated with turbulence from wind shear (MacIntyre et al., 2001) and convective mixing (Eugster et al., 2003), which affect CO_2 fluxes. Therefore, the separation of the epilimnion and hypolimnion due to thermal stratification is one of the most critical physical processes controlling C flux in lakes (Åberg et al., 2010; Andersen et al., 2019; Eugster et al., 2003).

Irradiance and thermal stratification affect chemical activity, biological activity, and physical transport in lakes (Imberger et al., 1985; Nakayama et al., 2012, 2019). Vertical mixing is an incredibly vital physical process in stratified lakes because it controls biochemical fluxes (Boehrer & Schultze, 2008; Gudasz et al., 2010; MacIntyre et al., 1993, 2002). River inflows and wind turbulence mix biotic and abiotic materials from sediments into the water column (Andersen et al., 2017; Boehrer & Schultze, 2008; Czikowsky et al., 2018; Hope et al., 2004; MacIntyre et al., 1993, 2002). Allochthonous C is the primary resource facilitating ecosystem production in lakes (Lu et al., 2018; McDonald et al., 2013; Vachon & del Giorgio, 2014). Thus, the hydrological effect on the vertical profile of DIC in a lake needs to be clarified by considering disturbances due to river inflows and wind. Water temperature is also a critical factor controlling the fate of C in shallow subtropical lakes. We thus investigated water temperature and DIC vertical profiles to quantify the seasonal mixing regime in Yuan-Yang Lake (YYL), Taiwan using the vertical profile of water temperature and DIC once or twice a month from July 2004 to December 2017. Furthermore, we investigated the seasonal patterns in the DIC vertical profiles to estimate net ecosystem production (NEP) in this shallow subtropical lake using a three-dimensional hydrological model.

2. Materials and Methods

2.1. Study Site

YYL is a typical shallow subtropical mountain lake in East Asia, located in the Chi-Lan area of Yilan County in northern Taiwan (24°57′ N, 121°40′E) at an altitude of about 1,650 m (Figure 1). YYL is a natural lake and has been registered as a long-term ecological study site by the National Science Council of Taiwan since 1992. Additionally, YYL has been a part of the global lake ecological observatory network (GLEON) since 2004. The air temperature around YYL ranges from −5 to 25°C and annual precipitation from 2,200 to 5,000 mm. For about 40% of the year, YYL is covered by heavy fog and receives a mean solar radiation of about 220 MJ m^{-2}. YYL has a surface area 3.6 ha and a water depth from 3.8 to 4.5 m, and, although it is in an alpine region, the lake surface is ice-free all year round. YYL is surrounded by pristine old-growth cypress forest, where the dominant tree species are *Chamaecyparis formosensis*, *Chamaecyparis obtusa* var. *formosana*, and *Rhododendron formosanum* Heiml. Aquatic plants exist in the lake, and *Sparganium fallax* and *Schoenoplectus mucronatus* subsp. *robustus* are the dominant species (Chou et al., 2000). The water surface color is brown and humic, with a mean pH of approximately 5.4 (Tsai et al., 2008; Wu et al., 2001). The

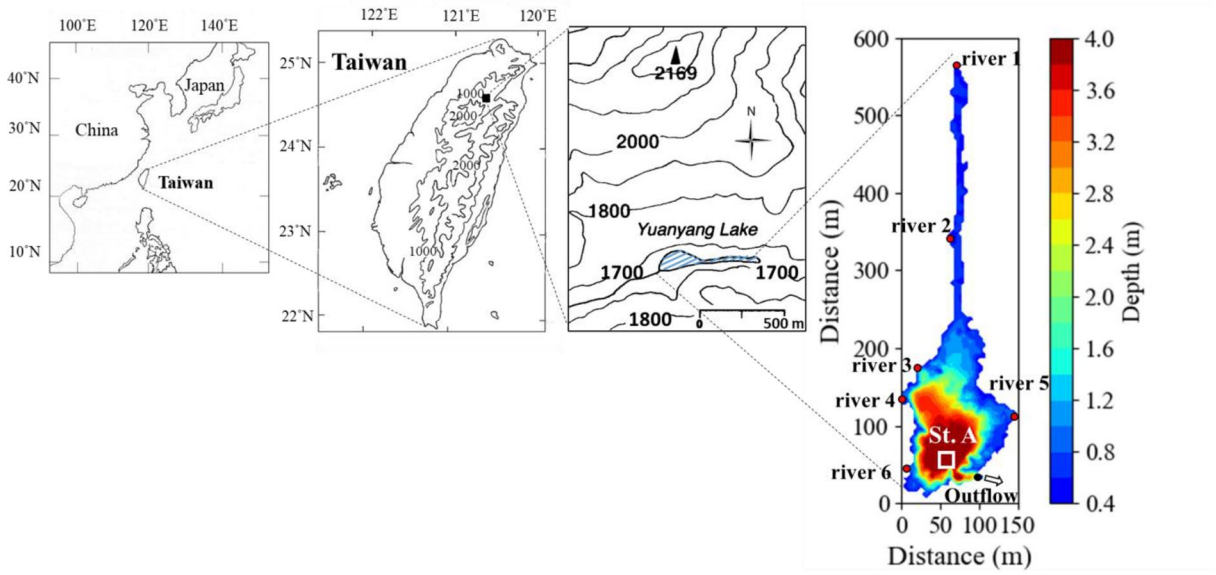

Figure 1. Location and bathymetry of Yuan-Yang Lake (YYL). White rectangle: St. A (the deepest part of the lake) where vertical profiles were taken. Red and black circles indicate inflow and outflow rivers, respectively.

water column is stratified from early April to October and is usually well-mixed in winter from December to February (Kimura et al., 2012; Tsai et al., 2008).

2.2. Data Collection

A buoy located at the deepest place (St. A) of the lake measured water temperature through the water column at 0.5-m increments, water depth (HOBO U20; Onset computer company), and wind speed 2 m above the lake surface every 10 min. A meteorological station within 1 km of the lake collected precipitation, air temperature, and atmospheric pressure measurements every 10 min. Water temperature was measured through the water column at water depths of 0.04, 0.25, 0.5, 0.75, 1.0, 1.5, 2, 2.5, 3.0, 3.5, and 4.0 m at St. A every 1 h using a thermistor chain (Templine, Apprise Technologies, Inc.,) (Figure 1). Total water depth was measured at St. A once or twice a month from July 2004 to December 2017. We also measured the water surface temperature (0.04 m) of six inflow rivers and one outflow river.

We sampled water at St. A at water depths of 0.04, 0.5, 1.0, 2.0 and 3.5 m once or twice a month. We also collected water samples at the water surface in six inflow rivers and one outflow river. The water samples were filtered with plastic filters (47 mm GF/F; Whatman) using a portable hand pump (Hand Vacuum pump, One Lincoln Way). The water samples were kept in airtight vials (Vial glass 40 ml, K60958A-912) and stored in a cooler box at around 4–10°C until DIC concentration measurements were taken (mg C L^{-1}), less than 72 h after sampling. We used a Total Organic Carbon (TOC) analyzer (O. I. TOC analyzer 1010 from 2004 to 2012 and model 1030 W/1088 from 2013 to 2017, Xylem) and persulfate digestion to detect DIC concentrations with an infrared gas detector. We employed a sonar (LMS-332c GPS Receiver and Sonar) to measure bathymetry in August 2007 with a spatial interval of 1.0 m, which was used in the three-dimensional hydrological model.

We categorized the year into four seasons: spring (March to May), summer (June to August), autumn (September to November), and winter (December to February). Since typhoons may cause significant disturbance to the stratification in summer and autumn, we added two more categories—summer typhoons (June to August) and autumn typhoons (September to November)—to explore how typhoons contribute to the vertical profile of water temperature and DIC. Note that the mean duration of typhoon events was less than a few days.

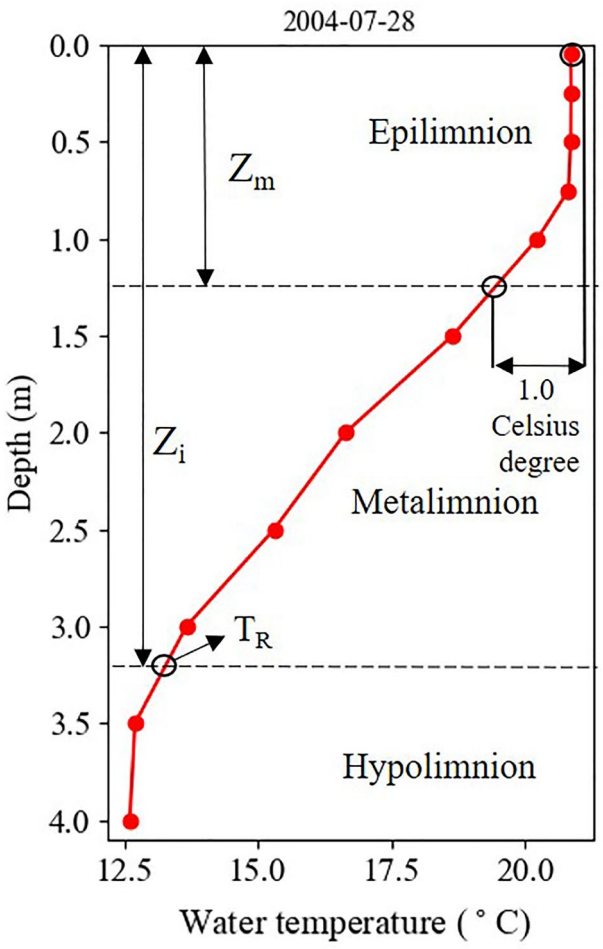

Figure 2. Definition of mixing depth (Z_m) and intrusion depth (Z_i). Vertical profile of water temperature on July 28, 2004.

2.3. Brunt–Väisälä Frequency, Mixing Depth, and Intrusion Depth

We used the Brunt–Väisälä frequency (N s^{-1}) to quantify the strength of stratification. The Brunt-Väisälä frequency is associated with vertical mixing in lakes (von Rohden & Ilmberger, 2001).

$$N = \sqrt{-\frac{g}{\rho}\frac{d\rho}{dz}} \tag{1}$$

where g is the gravity acceleration, ρ is the density of water, and z is the vertical coordinate of water depth (m). Since we calculated the vertical mean of N^2, we obtained $N^2 > 0$ for most cases.

To define the depth of vertical mixing, the mixing depth (Z_m, m) was calculated by following Staehr and Sand-Jensen (2007) (Figure 2).

$$Z_m = Z\big|_{T=T_S-1} \tag{2}$$

where Z_m is the mixing water depth, and T_S is the water surface temperature (at a depth of 0.04 m).

To estimate where river flow intrudes, we defined an intrusion depth (m), Z_i (Figure 2).

$$Z_i = Z\big|_{T=T_R} \tag{3}$$

where T_R is the water temperature of a river.

2.4. NEP

To estimate NEP, we used end-member analysis using the DIC of the rivers (Christophersen et al., 1990; Hooper et al., 1990). Since there are six inflow rivers in YYL, the mean DIC concentration (mg L^{-1}) of the inflow water was estimated as:

$$DIC_R = \frac{\sum_{i=1}^{6} Q_i DIC_i}{\sum_{i=1}^{6} Q_i} = \frac{\sum_{i=1}^{6} Q_i DIC_i}{Q_R} \tag{4}$$

where DIC_R is the mean DIC from rivers into YYL, DIC_i is the DIC from river$_i$, Q_i is the discharge from the river (Dalrymple, 1960; Laurenson, 1965), and Q_R is the total river discharge (m^3 s^{-1}). Q_1 to Q_6 were 0.072, 0.009, 0.027, 0.018, 0.036, and 0.018 m^3 s^{-1}, respectively.

The change in DIC (mg C m^{-3}) was modeled by applying a conceptual model (Nakayama, Komai, et al., 2020) as follows:

$$V_{total} C_U \frac{\partial DIC}{\partial t} = -V_{total} NEP + Q_{Re} C_U \left(DIC_R - DIC_L\right) - A_L F_{CO2} \tag{5}$$

where C_U is the coefficient that converts the unit from mg C L^{-1} to mg C m^{-3}, NEP is the NEP (mg C m^{-3} d^{-1}), V_{total} is the total volume of the lake (m^3), Q_{Re} is the effective exchange flux (m^3 d^{-1}), DIC_L is the mean DIC in YYL (mg L^{-1}), A_L is the lake surface area (m^2), and F_{CO2} is the DIC flux between the lake surface and atmosphere (mg C m^{-2} d^{-1}). Note that Q_{Re} is not generally equal to Q_R, so we needed to estimate Q_{Re} using a three-dimensional hydrological model.

Table 1
Equations and References for CO_2 flux (F_{CO2}) Across the Air-Water Interface

Variables	Equation	References & equipment
F_{CO2}	$k_{CO2} \cdot K_H \left(pCO2_{water} - pCO2_{air}\right)$	Fick's law diffusion
$pCO2_{air}$ (CO_2 partial pressure in the atmosphere)	Measured data. 390 (ppm)	Air pressure sensor (model 090D; Met One Ins., NW, USA)
$pCO2_{water}$	$\frac{DIC\left(10^{-pH}\right)^2}{\left[\left(10^{-pH}\right)^2 + \left(10^{-pH}\right)K_1 + K_1K_2\right]K_H}$	Cai & Wang, 1998
pH	Measured data	Water quality probe (Hydrolab 4α; Hach, CO, USA)
DIC	Measured data (DIC concentration, 0.04 m)	
k_{CO2} (Gas transfer velocity)	$k_{600}\left(\frac{Sc_{CO_2}}{600}\right)^{-0.67}$	Cole & Caraco, 1998
k_{600} (Gas exchange coefficient)	$2.07 + 0.215\,U_{10}^{1.7}$	Jähne et al., 1987
Sc_{CO_2} (Schmidt number)	$1911.1 - 118.11\,T + 3.4527\,T^2 - 0.04132\,T^3$	Wanninkhof, 1992
U_{10}	$U_2 \cdot \left(\frac{10_{(m)}}{2_{(m)}}\right)^{0.15}$	Smith, 1985
U_2	Measured data (Wind speed above water surface 2 m)	Wind monitor (model 05106; R.M. Young, MI, USA)
K_H (Henry's coefficient)	$\exp\left(108.39 + 0.0199\mathrm{T} - \frac{6920}{\mathrm{T}} - 40.452\log\mathrm{T} + \frac{669365}{T^2}\right)$	Plummer & Busenberg, 1982
K_1 (1st dissociation constant)	$\exp\left(-356.31 - 0.0609\mathrm{T} + \frac{21834}{\mathrm{T}} + 126.83\log\mathrm{T} - \frac{1684915}{\mathrm{T}^2}\right)$	Plummer & Busenberg, 1982
K_2 (2nd dissociation constant)	$\exp\left(-107.8 - 0.0325\mathrm{T} + \frac{5152}{\mathrm{T}} + 38.926\log\mathrm{T} - \frac{56371}{T^2}\right)$	Plummer & Busenberg, 1982
T	Measured data (Water temperature (K), 0.04 m)	

Note: Data were collected at St. A.

To understand how much inorganic C was released from the lake into the atmosphere and how C was exchanged between lake and atmosphere, we applied Fick's law to estimate the air-water CO_2 gas flux (Table 1). F_{CO2} is positive when CO_2 is emitted from the lake into the air.

We previously found that the change in DIC by air-water CO_2 gas exchange at the lake DIC level was negligible in Komuke Lagoon because of a large decrease in DIC due to photosynthesis by eelgrass (Nakayama, Komai, et al., 2020). However, YYL is a typical shallow subtropical lake, and its air-water CO_2 gas exchange is expected to be on the same order as NEP because phytoplankton is the dominant DIC sink and the biomass is much smaller than eelgrass. Therefore, we did not neglect the air-water CO_2 gas exchange in Equation 5. Although DIC_R changes considerably during a flood, the value of DIC_R becomes stable soon after the flood. Therefore, the fluctuation in DIC_R due to flooding is negligible when analyzing the seasonal change in NEP. Therefore, under the steady-state condition for DIC, NEP was obtained as:

$$\mathrm{NEP} = \frac{Q_{Re}}{\mathrm{V_{total}}} C_U \left(\mathrm{DIC}_R - \mathrm{DIC}_L\right) - \frac{A_L}{\mathrm{V_{total}}} F_{CO2} \tag{6}$$

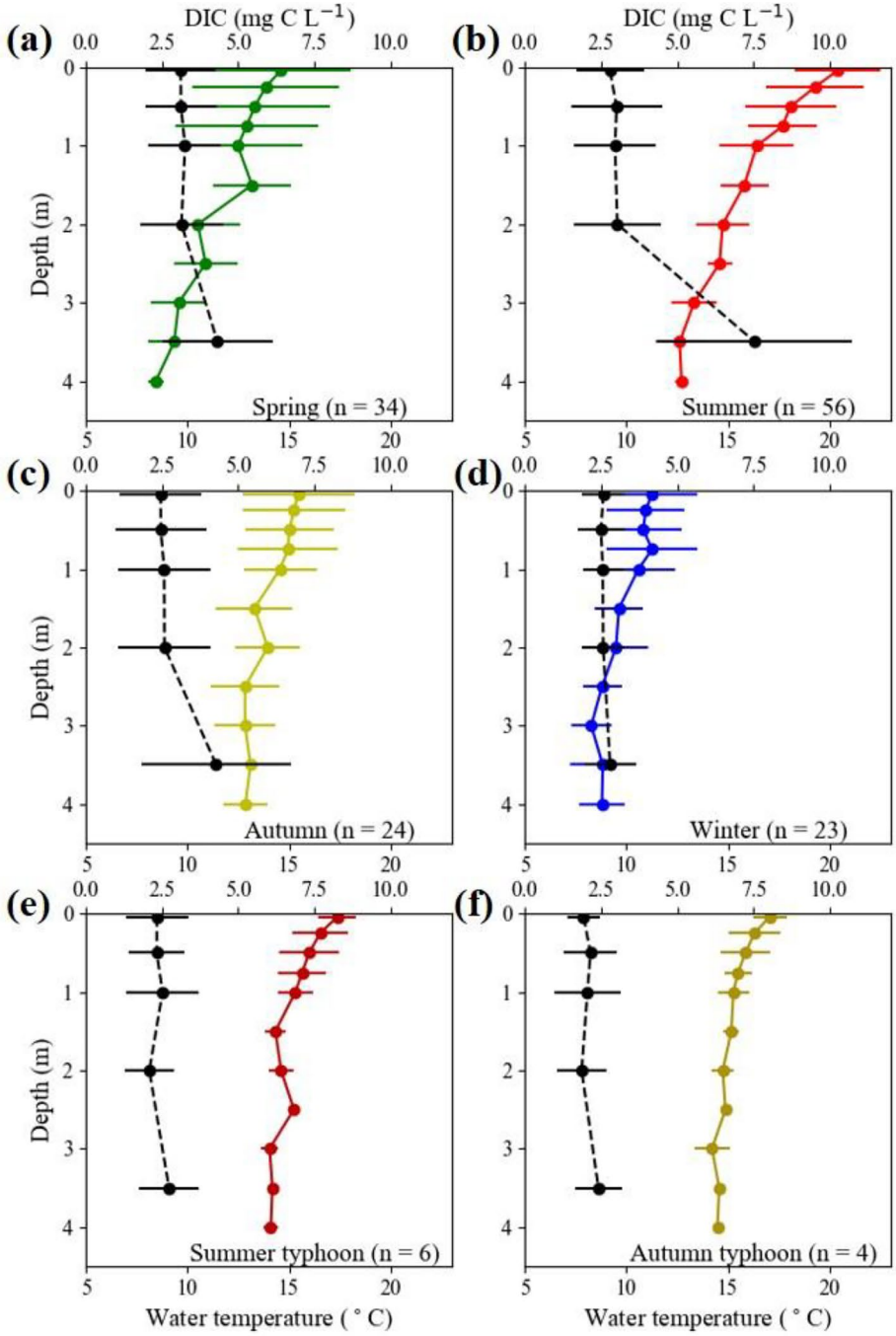

Figure 3. Vertical profiles of mean water temperature (colors solid lines) and dissolved inorganic C (DIC) (black dashes) in (a) spring, (b) summer, (c) autumn, and (d) winter, and during the (e) summer typhoons and (f) autumn typhoons from July 2004 to December 2017. The dots show the mean value, and the horizontal lines indicate the standard deviation (*n* is the number of samples).

When DIC_L is larger than DIC_R and CO_2 gas is released, inorganic *C* is produced in the lake, which leads to a negative NEP. When DIC_L is smaller than DIC_R and the CO_2 gas is absorbed, *C* is accumulated within the lake, which leads to a positive NEP. Note that the value of NEP is the sum of primary production and air-water CO_2 gas exchange (F_{CO2}).

We obtained ΔDIC in YYL using DIC at water depths of 0.04, 0.5, 1.0, 2.0, and 3.5 m.

$$\Delta DIC = \left(\Delta DIC_{0.04m} V_{0.04m} + \Delta DIC_{0.5m} V_{0.5m} + \Delta DIC_{1m} V_{1m} + \Delta DIC_{2m} V_{2m} + \Delta DIC_{3.5m} V_{3.5m}\right) / V_{total} \quad (7)$$

where V_{dep} is the volume (m^3) at a depth of *dep*, and ΔDIC_{dep} is the value of DIC at a depth of *dep*.

V_{total} / Q_{Re} corresponds to residence time in YYL (Nakayama, Komai, et al., 2020). In general, residence time is not equal to V_{total} / Q_R because the stratification affects a three-dimensional flow and mass transport. Therefore, we attempted to estimate residence time using a three-dimensional numerical simulation. Finally, we obtained NEP by introducing $\Delta DIC = DIC_L - DIC_R$ as:

$$NEP = -C_U \frac{\Delta DIC}{t_r} - \frac{A_L}{V_{total}} F_{CO2} = -C_U \frac{\Delta DIC}{t_r} - F_C \quad (8)$$

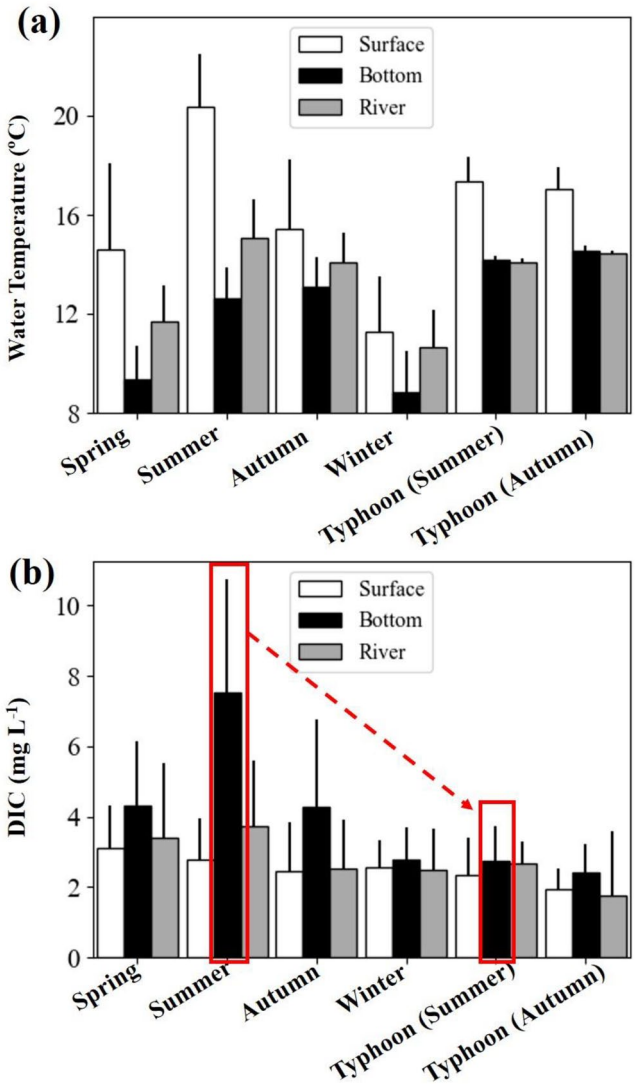

Figure 4. Comparison of (a) water temperatures and (b) dissolved inorganic C (DIC) of the water surface (0.04 m, white bars), water bottom (3.5 m, black bars), and river water (T_R and DIC_R, gray bars). The bars represent the mean values, the solid black lines indicate the standard deviations, and red rectangles indicate the change in surface DIC concentration due to dilution after typhoons in summer.

where t_r is the residence time (d^{-1}) of YYL.

To estimate the residence time in YYL, we performed three-dimensional hydrological simulations using a three-dimensional environmental model, Fantom, which is based on object-oriented programming methods (Laniak et al., 2013; Maruya et al., 2010; Nakamoto et al., 2013; Nakayama et al., 2014, 2016; Nakayama, Sato, et al., 2020; Nakayama, Shintani, et al., 2020). To evaluate bathymetry's effects on the flow field and residence time, we used a Fantom to simulate the bottom slope in a *z* coordinate system with partial cells (Adcroft, 1997). A generic length-scale (GLS) equation model was also employed to evaluate how the vertical mixing affected the water's mass and energy transport (Jones & Launder, 1972; Umlauf & Burchard, 2003). For numerical simulations, the initial vertical profiles of mean water temperatures and DIC for each season were obtained by applying typical stratified conditions (Figure 3). The horizontal grid size was 4.0 m, and the vertical grid size was 0.2 m. The time step was 0.5 s.

The residence time (t_r) was estimated from the temporal change in mean tracer concentrations in the entire domain of YYL. Initially, we used a uniform tracer concentration of 1.0 for the entire domain of YYL. Then, we computed the time series of the mean tracer concentration, which was used to estimate residual time using:

$$Tr = Tr_0 \exp\left(-\frac{t}{t_r}\right) \quad (9)$$

where Tr is the mean tracer concentration for the entire domain of YYL, Tr_0 (= 1.0) is the initial mean tracer concentration, and t is the time (d^{-1}).

3. Results

3.1. Water Temperature and DIC in YYL

Mean water surface temperature was the highest in summer (19.1°C), and the difference in water temperature between the water surface (0.04 m) and bottom (4.0 m) was around 10.8°C (Figure 3b). Mean water surface temperature was lowest in winter (11.3°C) (Figure 3d). Mean water temperatures adjacent to the bottom were 8.5, 12.7, 12.9, and 8.7 °C for spring, summer, autumn, and winter, respectively (Figures 3a–3d). The mean surface water temperatures were lower during the summer typhoons than the average summer conditions, but mean surface water

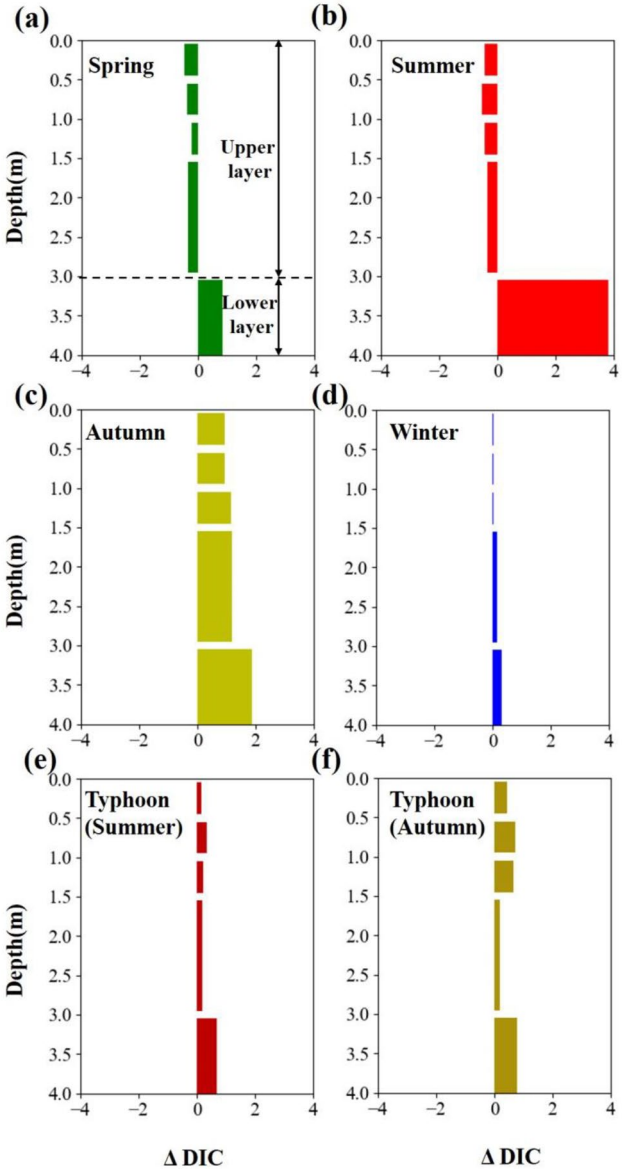

Figure 5. Mean vertical profiles of ΔDIC (mg C L^{-1}) in (a) spring, (b) summer, (c) autumn, (d) and winter, and during the (e) summer typhoons, and (f) autumn typhoons.

temperatures during the autumn typhoons were higher than normal autumn conditions (Figures 3b, 3c, 3e, and 3f).

Mean surface water DIC was about 3.0 mg C L^{-1} from spring to summer and about 2.5 mg C L^{-1} from autumn to winter (Figures 3a–3d). Mean surface water DIC was lowest during the autumn typhoons (Figures 3e and 3f). YYL stored larger amounts of DIC in the hypolimnion (3.5 m) than surface waters from spring to autumn (Figures 3a–3c). Mean hypolimnion DIC was highest in summer (7.5 mg C L^{-1}), although the mean DIC during the summer typhoons were vertically uniform and only about 2.5 mg C L^{-1} (Figures 3b and 3e). Mean hypolimnion DIC was also low in winter (2.8 mg C L^{-1}), due to vertical mixing and the low prevailing water temperatures (Figure 3d). The vertical profile of mean DIC was almost uniform after typhoons (Figures 3e and 3f).

Mean river temperatures were the highest in summer, at 15.1°C, and lowest in winter, at 10.7°C (Figure 4a). The difference in water temperature between lake surface water and the rivers was at its highest in summer. River DIC in spring and summer was also higher than at other times (Figure 4b). Mean river DIC was highest in summer (3.7 mg C L^{-1}) and lowest (1.8 mg C L^{-1}) during the autumn typhoons (Figure 4b). Mean DIC concentration declined approximately 40% after the typhoons (red rectangles in Figure 4b).

The absolute mean of ΔDIC in the upper layer was lower in spring and summer than in autumn (Figures 5a–5c). Mean lower layer ΔDIC in spring (0.83 mg C L^{-1}) was lower than that autumn (1.86 mg L^{-1}), and mean ΔDIC was highest in summer (3.82 mg C L^{-1}). Mean ΔDIC in the upper layer was highest in autumn (around 1.0 mg C L^{-1}), while the absolute value of mean ΔDIC was the lowest in winter (about 0.06 mg L^{-1}) (Figures 5c and 5d). Mean upper layer ΔDIC was smaller in summer than during the summer typhoons (Figures 5b and 5e). In contrast to summer, mean upper layer ΔDIC in autumn was larger than during the autumn typhoons (Figures 5c and 5f).

3.2. Mixing Depth, Brunt-Väisälä Frequency, and Intrusion Depth

Mixing depths were less than 25% of the total water column for all categories (Figure 6a). Mean mixing depth was the greatest in winter (25% of the water depth) and smallest in summer (7.50%; Figure 6a). Mean Brunt-Väisälä frequency ranged from around 6.00×10^{-3} to 1.30×10^{-2} s^{-1}; in summer, it was twice as much as when it was at its lowest in autumn (Figure 6b). In other words, the stratifications in spring and summer were stronger than those in autumn and winter. The Brunt-Väisälä frequency after typhoons was higher than in autumn and winter because we conducted field observations a few days after a typhoon passed and stratification formed due to sunny weather (Figure 6b). Mean intrusion depth was about 50% of the total water column from spring to autumn, and 100% of the whole water column after the typhoons (Figure 6c). In contrast, intrusion depth in winter was small, approximately 10% of the total water column (Figure 6c).

Water surface DIC was not associated with water surface temperature (Figure 7a). However, hypolimnion DIC and water temperature showed a significant positive correlation ($rs = 0.61$, $p < 0.001$) (Figure 7b). Hypolimnion DIC and river DIC had the strongest positive correlation ($rs = 0.69$, $p < 0.001$) (Figure 7c). Hypolimnion DIC and river DIC showed a positive correlation with Brunt-Väisälä frequency

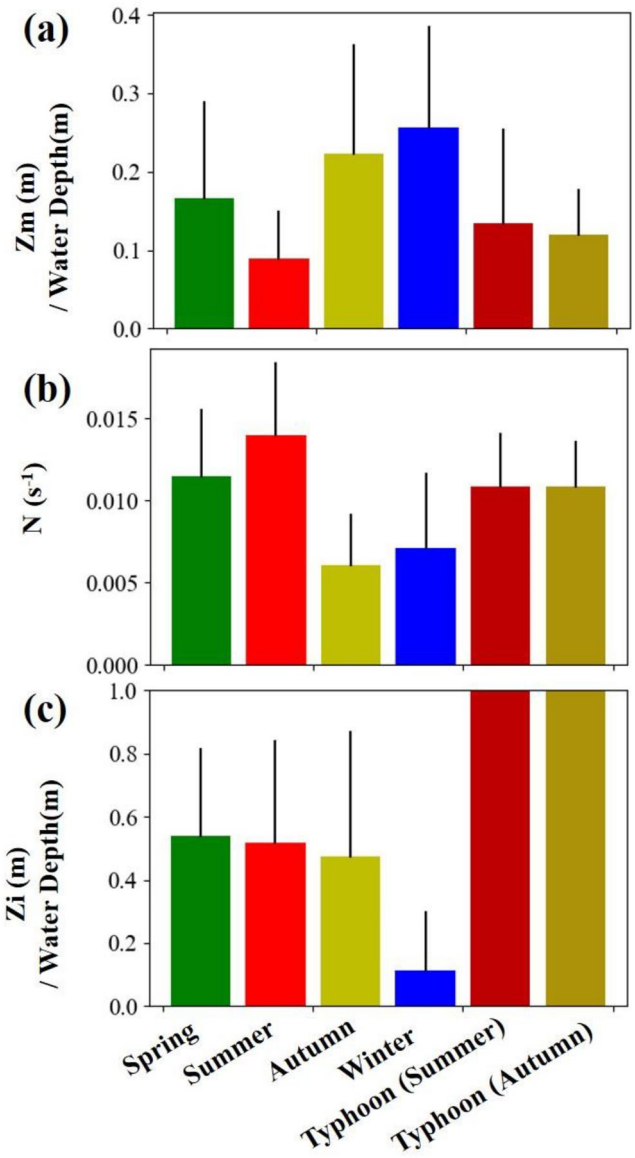

Figure 6. Comparison of the (a) mixing depth (Z_m), (b) Brunt–Väisälä frequency (N), and (c) intrusion depth (Z_i) for each category in Yuan-Yang Lake (YYL). The bars represent the mean values, and the solid black lines indicate the standard deviations. The total water depths were used to normalize the intrusion and mixing depths.

(rs = 0.43 and 0.32, $p < 0.001$) (Figures 7e and 7f), but water surface DIC was not clearly associated with water temperature or Brunt-Väisälä frequency (Figures 7a and 7d). The Brunt-Väisälä frequency and mixing depth were associated with surface water temperatures (Figures 7g and 7h) with high Spearman correlation coefficients (rs = 0.64 & 0.40, $p < 0.001$). Although Brunt-Väisälä frequency and mixing depth had the strongest absolute correlation (rs = −0.88, $p < 0.001$) (Figure 7i), mixing depth was not strongly correlated with hypolimnion DIC or river DIC (Table 2). Intrusion depth had significant positive correlations with water surface temperature, Brunt-Väisälä frequency, and hypolimnion DIC (rs = 0.58, 0.32, and 0.32, respectively, $p < 0.001$). In contrast, intrusion depth was not associated with mixing depth, water surface DIC, or river DIC.

3.3. NEP and F_{CO2} in YYL

To demonstrate the effect of stratification on vertical mixing, Figure 8 shows the vertical distribution of tracers under summer conditions. River flow intrudes into the middle layer in YYL due to stratification, and the upper layer is well-mixed on the second day after the initial condition (Figures 8a and 8b). However, it was found that the river flow cannot intrude into the lower layer directly because the water temperature of the river inflow is almost the same as that of the thermocline, resulting in the slow descent of the thermocline from the second to the third day (Figure 8c). In contrast, the tracer was confirmed to be well-mixed in the entire domain in winter because of weak stratification. Finally, the residence time (t_r) in spring, summer, autumn, and winter was 2.6, 2.6, 1.7, and 1.3 days, respectively. The residence time was longer in spring and summer than autumn and winter because spring and summer have a stronger stratification than autumn and winter. The residence time in winter was the shortest (1.3 days).

In general, residence time is determined by inflow and stratification. Even though the rainfall intensity is higher in summer and autumn than spring and winter, the inflow returns to the base flow immediately after the typhoons cease. Therefore, we assumed that the inflow was constant between seasons, and thus expected there to be no direct influence of precipitation on residence time at the seasonal timescale. On the other hand, a previous study found that typhoons (precipitation) caused vertical mixing of the water column for up to 7–10 days after the typhoons (Tsai et al., 2011). Although the average irradiance (solar radiation) intensity was similar between spring and autumn, the stratification in autumn tended to be weaker than spring due to the vertical mixing induced by the typhoons. In summer, irradiance was the strongest, resulting in the strong stratification, despite the typhoons. The large density difference between the upper and lower layers inhibited the penetration of river inflow into the hypolimnion. Thus, in spring and summer, the exchange of water between the upper and deeper layers was suppressed. Consequently, the residence time was longest in summer and spring, followed by autumn, and was shortest in winter.

Mean CO_2 emissions ranged from 31.7 to 50.2 mg C m^{-3} d^{-1}, and mean pCO_{2water} was around 564–662 μatm (Table 3). Water temperatures (11.1 ± 1.9 C), DIC (2.20 ± 0.43 mg L^{-1}), and $\boldsymbol{k_{CO2}}$ (1.85 ± 0.42 m s^{-1}) were lowest in winter, which led to a lower mean $\boldsymbol{F_{CO2}}$ than in spring and autumn. Mean $\boldsymbol{F_{CO2}}$ was lowest in summer (131.2 mg CO_2 m^{-2} d^{-1}).

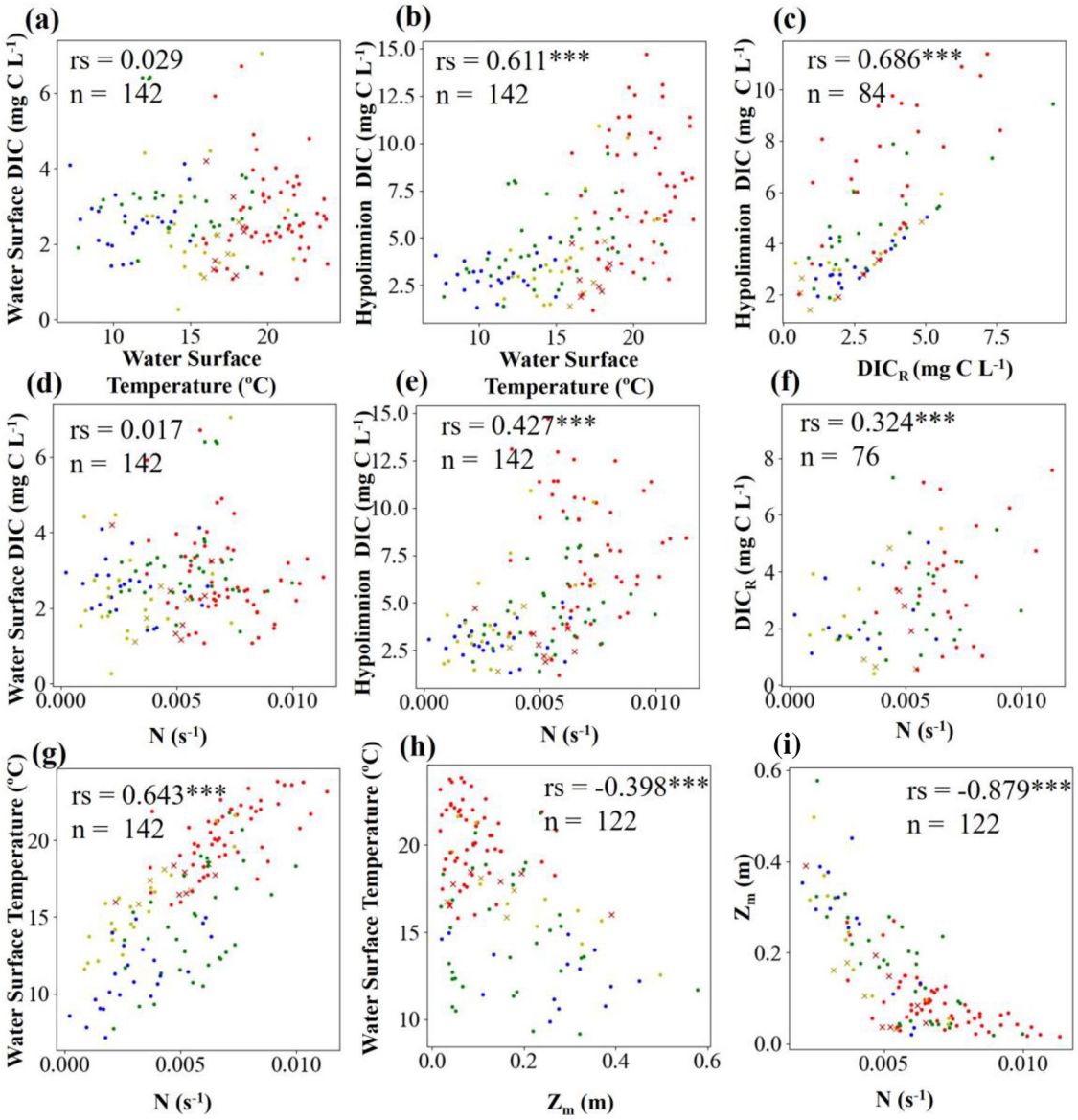

Figure 7. Relationships between (a) water surface temperature and water surface dissolved inorganic C (DIC), (b) water surface temperature and hypolimnion DIC, (c) river DIC (DIC_R) and hypolimnion DIC, (d) Brunt–Väisälä frequency (N) and water surface DIC, (e) N and hypolimnion DIC, (f) N and DIC_R, (g) N and water surface temperature, (h) mixing depth (Z_m) and water surface temperature, and (i) N and Z_m. The green, red, yellow, and blue points represent spring, summer, autumn, and winter data, respectively. The dark red and dark yellow crosses represent the summer and autumn typhoon data. rs is the Spearman correlation coefficients. ***Indicates statistical significance at *p*-value ≤0.001.

From the viewpoint of the entire lake, NEP was positive only in spring (Figure 9). Since the upper layer plays a major role in CO_2 emissions, we applied (8) to estimate NEP in the upper layer using the ΔDIC , t_r and the volume in the upper layer. As a result, NEP in the upper layer was 114.1, 144.0, −644.8, and −69.7 mg C m^{-3} d^{-1} in spring, summer, autumn, and winter, respectively. The effect of stratification on the suppression of vertical mixing between the upper and lower layers enhanced positive NEP in spring and summer. In contrast, NEP in the lower layer was −319.6, −1,470.3, −1,282.6, −374.5 mg C m^{-3} d^{-1} in spring, summer, autumn, and winter, respectively, which provides evidence of C production in the lower layer. The contribution of F_C to NEP in the upper layer was 24.9%, 15.5%, 5.5%, and 33.5% in spring, summer, autumn, and winter, respectively (Table 3). Therefore, CO_2 emissions were confirmed to not be negligible in (8).

Table 2
Spearman Correlation Coefficients for DIC, Water Surface Temperature, Brunt-Väisälä Frequency, Mixing Depth, and Intrusion Depth

Variables	Mixing depth	Brunt-Väisälä frequency	Water surfaceDIC	Hypolimnion DIC	River DIC	Intrusion depth
Water surface temperature	−0.398***	0.643***	0.029	0.611***	0.310**	0.581***
	(122)	(142)	(142)	(142)	(76)	(66)
Mixing depth		−0.879***	0.115	−0.221	−0.158	−0.155
		(122)	(122)	(122)	(66)	(52)
Brunt-Väisälä frequency			0.017	0.427***	0.324***	0.324***
			(142)	(142)	(76)	(66)
Water surface DIC				0.438***	0.320***	0.162
				(152)	(84)	(66)
Hypolimnion DIC					0.686***	0.321***
					(84)	(66)
River DIC						−0.005
						(31)

*Represents the Statistical Significance at p-value ≤ 0.05.
**Represents the Statistical Significance at p-value ≤ 0.01.
***Represents the Statistical Significance at p-value ≤ 0.001.

4. Discussion

Stratification was confirmed to be stronger in spring and summer (mean N: 0.011 s^{-1} & 0.013 s^{-1}, respectively) than autumn and winter (mean N: 6.00×10^{-3} s^{-1} & 7.00×10^{-3} s^{-1}, respectively) in YYL (Figures 3 and 6). Strong stratification inhibited vertical DIC transport from the lower to the upper layer, which resulted in negative ΔDIC in the upper layer from spring to summer due to the predominance of photosynthesis (Figure 5). Spearman correlations showed strong correlations between the Brunt-Väisälä frequency and hypolimnion DIC (Figure 7e). Strong thermal stratification during spring and summer drove longer residence times than in autumn and winter. NEP in the upper layer was positive due to the stratification in spring and summer, and NEP in the upper layer dramatically decreased from summer to autumn due to weak stratification (Figure 9). Therefore, DIC produced in the lower layer was vertically transferred easily to the water surface in autumn, which resulted in the highest CO_2 emissions in YYL (Table 3). Since ecological production was the lowest in winter due to the low water temperature, the absolute value of NEP in the upper layer was smaller in winter than autumn (Figure 9).

Average wind speeds were 0.70 ± 0.33, 1.15 ± 0.8, 1.11 ± 0.76, and 1.07 ± 0.51 m s^{-1} in spring, summer, autumn, and winter, respectively. Previous studies showed that wind shear induces turbulent mixing in YYL (Kimura et al., 2012, 2014, 2017). However, we found that wind shear was not a key driver of vertical mixing on a seasonal scale. We compared the numerical simulations with and without wind stress and found that inflow is one of the main factors controlling residence time. Therefore, although the averages and standard deviations of wind speed from summer to autumn were higher than those in spring and winter, the residence times were mainly controlled by the intrusion depth of river flow, not wind speeds. Stratification in spring and summer is stronger than in autumn and winter. In summer and spring, since the river water temperature is similar to that of the metalimnion and is higher than in the hypolimnion, river inflows were constrained in the metalimnion (Figures 10a and 10b). Thus, the river intrusion cannot penetrate the hypolimnion because of the lake's strong stratification. In this case, only partial vertical mixing occurs between the metalimnion and epilimnion. Consequently, it takes longer to renew hypolimnion water with river inflows. In contrast, river water temperature is similar to that of the metalimnion or epilimnion (upper layer), and river inflows intrude into the upper layer in autumn and winter (Figures 10c and 10d). Even though the intrusion occurs adjacent to the water surface or metalimnion, whole-lake mixing occurs because stratification is weeker and vertical mixing is less suppressed. Thus, autumn and winter have a shorter residence time compared to spring and summer, and stratification plays a key role in controlling the

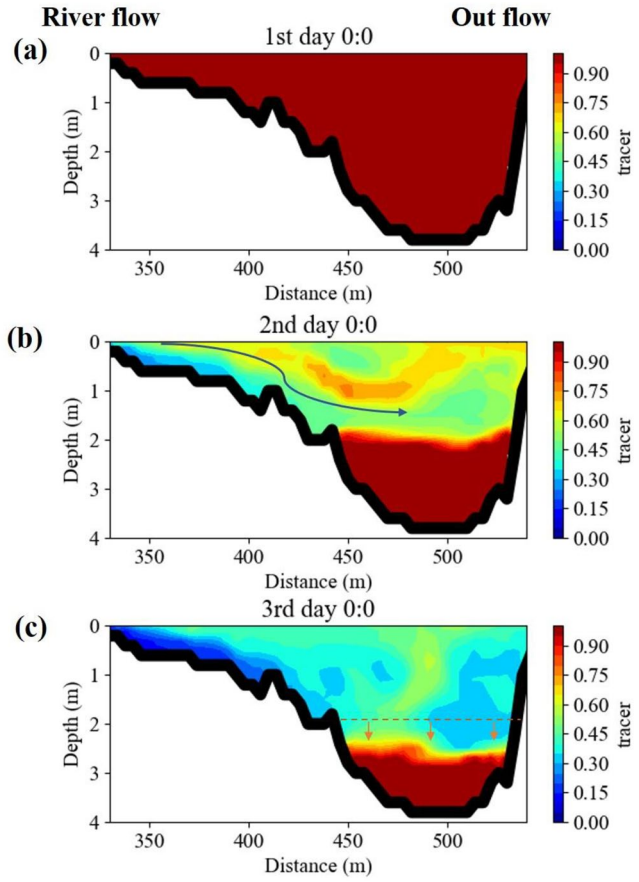

Figure 8. Vertical distribution of the tracer in summer. (a) Day 1, 00:00 a.m.; (b) day 2, 00:00 a.m.; (c) day 3, 00:00 a.m. The horizontal coordinate shows the distance from the northernmost point of YYL (m); the vertical coordinate shows the depth (m) from the water surface to the bottom. Contour shows the concentration of the tracer.

water renewal within lakes. This role can be evaluated precisely using a three-dimensional numerical simulation. This role can be evaluated precisely using a three-dimensional numerical simulation; this simulation method is more accurate for estimating residence time than the method that used the total volume of a lake and river inflow.

Previous studies demonstrated that thermal stratification was a significant driver of pCO_2 and CO_2 fluxes (Åberg et al., 2010; Andersen et al., 2019; Vachon & del Giorgio, 2014). Precipitation and storm events played a particularly vital role when they flushed large terrestrial DIC concentrations into the lake, which then released CO_2 and CH_4 (Bartosiewicz et al., 2015; Hope et al., 2004; Tonetta et al., 2017; Vachon & del Giorgio, 2014). There were 10 typhoon events in our data set, all of which occurred in summer and autumn (Table 4). Although the strength and frequency of typhoons were different between summer and autumn (Table 4), our results showed that the vertical profile of DIC and water temperature reflected a weak stratification after all typhoons (Figures 3b, 3c, 3e, and 3f). Each typhoon event led to considerable precipitation and river discharge events relative to the annual precipitation, so the stratification became very weak after each typhoon (Figures 3e and 3f). Kimura et al. (2012) applied the lake number (von Robertson & Imberger, 1994, L_N) to quantify the vertical mixing in YYL, and suggested that the water column was well-mixed ($L_N < 1$) during typhoons and the winter. Wind shear and convective mixing play a large role in diurnal heat flux in lakes (Imberger, 1985). When typhoons mixed the water column, the heat flux from the air into the lake decreased dramatically in YYL (Kimura et al., 2014). Czikowsky et al. (2018) demonstrated that the duration of well-mixed conditions due to storms was around 1–2 days in Lake Pleasant, which resulted in a 50% decrease in heat flux compared with the strongly stratified period. Previous studies suggested that storm events may impact CO_2 fluxes (Liu et al., 2016; Tonetta et al., 2017; Vachon & del Giorgio, 2014). CO_2 emissions across the air-water interface due to seasonal cooling-induced mixing are larger than those due to storm-induced mixing (Czikowsky et al., 2018). Our analysis revealed that CO_2 emissions peaked in autumn because the water column is less stratified then. These suggest that ty-

Table 3
CO_2 flux in YYL From July 2011 to December 2017 (not Including 2,012 and 2,013)

Variables and unit	Spring	Summer	Autumn	Winter
N	12	18	12	12
WT (°C)	15.59 ± 2.96	20.58 ± 1.87	15.72 ± 2.18	11.05 ± 1.92
k_{CO2} (m s^{-1})	2.23 ± 0.55	2.42 ± 0.33	2.35 ± 0.26	1.85 ± 0.42
pH	6.10 ± 0.84	5.78 ± 0.85	6.05 ± 0.58	6.25 ± 0.66
DIC (mg L^{-1})	2.44 ± 0.54	2.31 ± 1.32	2.56 ± 1.70	2.20 ± 0.43
$pCO2_{air}$ (μatm)	331.6 ± 1.30	331.6 ± 1.05	332.4 ± 0.79	332.0 ± 0.52
$pCO2_{water}$ (μatm)	634.3 ± 147.1	563.7 ± 328.3	661.8 ± 429.3	608.8 ± 116.9
F_{CO2} (mg CO_2 m^{-2} d^{-1})	167.3 ± 70.1	131.2 ± 186.2	207.4 ± 290.8	139.9 ± 62.9
F_C (mg C m^{-3} d^{-1})	28.49 ± 11.94	22.35 ± 31.71	35.32 ± 49.53	23.83 ± 10.71

Note. Fc is CO_2 emission.

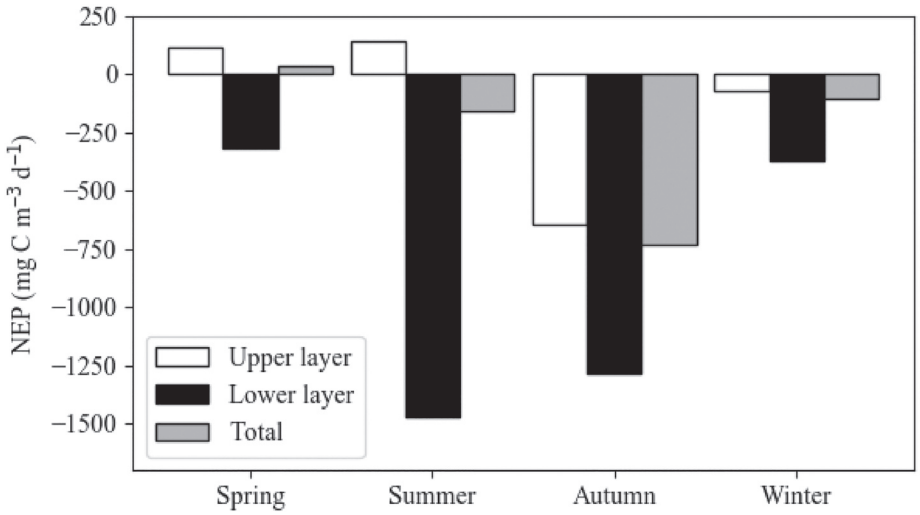

Figure 9. Net ecosystem production (NEP) in Yuan-Yang Lake (YYL). C is absorbed when NEP > 0 and C is released when NEP < 0. White bars represent NEP in the upper layer (0.04–2.5 m water depth), black bars represent NEP in the lower layer (2.5–4.0 m water depth), and gray bars represent the whole-lake mean NEP.

phoons may facilitate the vertical mixing of the lake. Consequently, it is necessary to consider the long-term effects of typhoons on CO_2 emissions, even to analyze seasonal changes in CO_2 emission.

CO_2 emissions in YYL were confirmed to be similar to other shallow temperate lakes that ranged from 131.2 to 207.4 mg CO_2 m^{-2} d^{-1} (Aufdenkampe et al., 2011; Raymond et al., 2013). In particular, mean $\boldsymbol{F_{CO2}}$ was lowest in summer because of the strong stratification (Figures 3b and 6b, and Table 3). Our results showed that mean $\boldsymbol{F_{CO2}}$ was highest in autumn (207.4 mg CO_2 m^{-2} d^{-1}) due to the supply of DIC from the lower to the upper layer under conditions of weak stratification (Figures 3c and 5c). The large standard deviation of DIC from summer to autumn was associated with a large standard deviation in $\boldsymbol{F_{CO2}}$ due to high-frequency typhoons (Tables 4). Therefore, we suggest that both extensive loading of allochthonous C from the

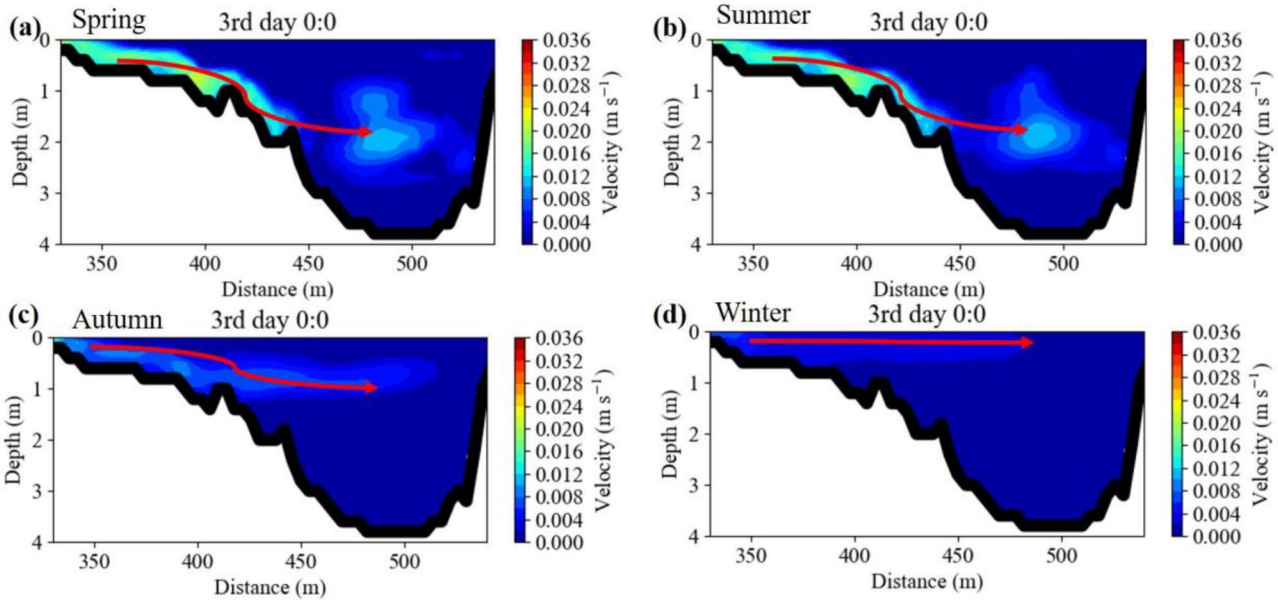

Figure 10. Vertical distribution of horizontal velocities on day 3 (00:00 a.m.) in (a) spring, (b) summer, (c) autumn, and (d) winter. The horizontal coordinate shows the distance from the northernmost point of Yuan-Yang Lake (YYL) (m); the vertical coordinate shows the depth (m) from the water surface to the bottom. Contour shows the horizontal velocity (m s^{-1}).

Table 4
Characteristics of Precipitation and Wind Speed of Summer and Autumn Typhoons From 2004 to 2017

Typhoon name	Date	Sampling date	Total precipitation (mm)	Maximum daily precipitation (mm)	Maximum wind speed (m s^{-1})	Ranking
Summer typhoons (Total 56 typhoon events)						
201513SOUDELOR	August 7–9, 2015	-	355.5	304.0	49.7	3rd/81
200708SEPAT	August 16–19, 2007	August 22–24, 2007	266.2	129.6	27.8	16th/81
200417AERE	August 23–26, 2004	August 31, 2004	283.9	232	34.1	4th/81
200509MATSA	August 3–6, 2005	August 9, 2005	227.4	127	31.2	18th/81
200505HAITANG	July 16–20, 2005	July 20, 2005	248.7	120.5	36.8	20th/81
Autumn typhoons (Total 25 typhoon events)						
200813SINLAKU	September 12–15, 2008	September 20, 2008	552	355.5	44.7	2nd/81
201013MEGI	October 21–23, 2010	October 25, 2010	501.9	356.5	16.6	1st/81
200513TALIM	September 1, 2005	September 5, 2005	149	149	39.5	13th/81
200712WIPHA	September 17–18, 2007	September 20, 2007	85.3	59.5	16.3	33rd/81

Note. The data come from the typhoon database of the Central Weather Bureau in Taiwan. The meteorological station is located in Yilan CWBT station (24°76′39″ N, 121°75′65"' E). The ranking uses maximum daily precipitation of typhoons events. 201513SOUDELOR was the best ranking in summer.

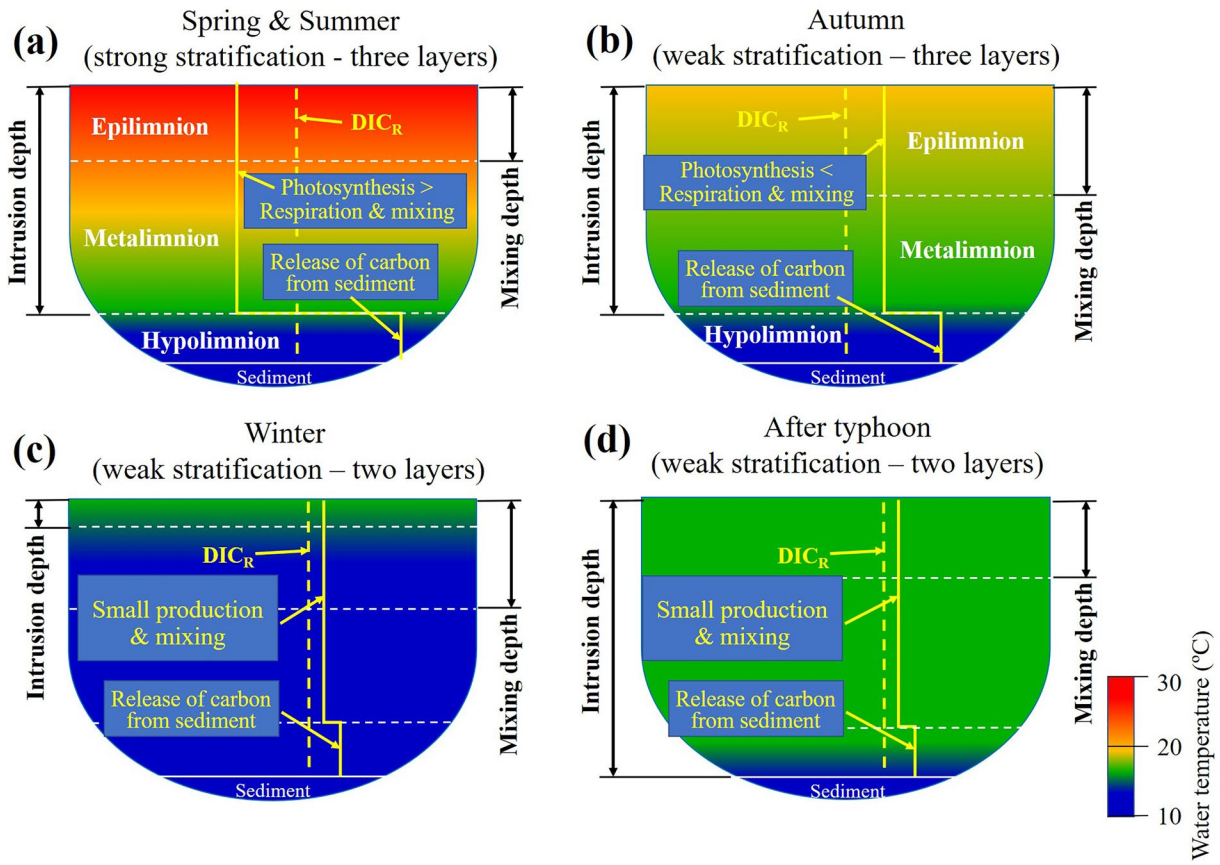

Figure 11. Schematic diagrams of stratification and DIC_R in (a) spring and summer, (b) autumn, (c) winter, and (d) after typhoons. The horizontal white-dash lines represent the thermocline, the vertical yellow lines represent the DIC_L, and the vertical yellow-dash lines represent DIC_R.

surrounding forest and storm events seasonally influence CO_2 emissions from shallow lakes (Chiu et al., 2020; Hope et al., 2004; Shade et al., 2010; Sobek et al., 2003; Tsai et al., 2008).

5. Conclusions

We developed a NEP model by successfully including the air-water CO_2 gas exchange and the stratification effect. The residence time was confirmed to be vital information for estimating NEP in a subtropical lake. We categorized the seasonal pattern of stratification in a shallow subtropical lake (summarized in Figure 11). Stratification is most intense in spring and summer, forming an apparent three-layer system. Although hypolimnion DIC is very high due to the release of sediments from the lake bottom, strong stratification inhibits the vertical mixing of hypolimnion DIC into the epilimnion. As a result, DIC in the upper layer tends to be lower due to photosynthesis. Although mean air temperatures in autumn were almost the same as in spring, stratification was weaker due to vertical mixing by typhoons. DIC tended to be uniform from the lower to the upper layer. In contrast, the water column is weakly stratified in winter, and river flow intrudes in a layer adjacent to the water surface. Foggy conditions reduced solar radiation in winter to less than about 150 J m^{-2}, low water temperatures and light limitation affect ecosystem production, and cold and dark conditions are expected to lead to little biological activity. Therefore, it is critical to factor in the effects of stratification when estimating the DIC and NEP dynamics in a lake. In general, stratification formation depends not only on river inflow, but also wind stress, lake size, and water depth. All these factors affect the generation of upwelling and internal waves, such as found with the Coriolis effect. Consequently, we suggest that future studies include a detailed three-dimensional numerical model to improve the accuracy of CO_2 gas exchange estimations in lakes.

Data Availability Statement

The executable binary (Windows, Mac, Linux) for the three-dimensional hydrodynamic model, Fantom, used in this study is available from http://www.comp.tmu.ac.jp/shintani/fantom.html. The model outputs are available from https://doi.org/10.5281/zenodo.3900032, "The model outputs."

Acknowledgments
This work was supported by the Taiwan National Science Council, Taiwan (NSC 94-2621-B-001-003, NSC 95-2621-B-001-001, and 97-2621-B-039-001-MY2), Ministry of Science and Technology, Taiwan (MOST 105-2621-B-039-001, MOST 107-2621-M-239-001), Academia Sinica, Taiwan (AS-103-TP-B15) for CY Chiu; China Medical University, Taiwan (CMU108-S-26 and CMU109-S-16) for JW Tsai; and the Japan Society for the Promotion of Science under grant 18H01545 and 18KK0119 for K Nakayama. The authors thank BS Lin, YL Chou, YS Hsueh, JY Liu, YX Lan, ZY Wu, YJ Miao, and LC Jiang for their help with water sample collection and chemistry analysis. This study benefited from participation in the Global Lakes Ecological Observatory Network (GLEON).

References

Åberg, J., Jansson, M., & Jonsson, A. (2010). Importance of water temperature and thermal stratification dynamics for temporal variation of surface water CO_2 in a boreal lake. *Journal of Geophysical Research*, *115*, G02024. https://doi.org/10.1029/2009JG001085

Adcroft, A., Hill, C., & Marshall, J. (1997). Representation of topography by shaved cells in a height coordinate ocean model. *Monthly Weather Review*, *125*, 2293–2315. https://doi.org/10.1175/1520-0493(1997)125<229310.1175/1520-0493(1997)125<2293:rotbsc>2.0.co;2

Andersen, M. R., Kragh, T., Martinsen, K. T., Kristensen, E., & Sand-Jensen, K. (2019). Correction to: The carbon pump supports high primary production in a shallow lake. *Aquatic Sciences*, *81*(2), 24. https://doi.org/10.1007/s00027-019-0625-4

Andersen, M. R., Sand-Jensen, K., Iestyn Woolway, R., & Jones, I. D. (2017). Profound daily vertical stratification and mixing in a small, shallow, wind-exposed lake with submerged macrophytes. *Aquatic Sciences*, *79*(2), 395–406. https://doi.org/10.1007/s00027-016-0505-0

Aufdenkampe, A. K., Mayorga, E., Raymond, P. A., Melack, J. M., Doney, S. C., Alin, S. R., et al. (2011). Riverine coupling of biogeochemical cycles between land, oceans, and atmosphere. *Frontiers in Ecology and the Environment*, *9*(1), 53–60. https://doi.org/10.1890/100014

Bade, D. L., Carpenter, S. R., Cole, J. J., Hanson, P. C., & Hesslein, R. H. (2004). Controls of δ13 C-DIC in lakes: Geochemistry, lake metabolism, and morphometry. *Limnology & Oceanography*, *49*(4), 1160–1172. https://doi.org/10.4319/lo.2004.49.4.1160

Bartosiewicz, M., Laurion, I., & MacIntyre, S. (2015). Greenhouse gas emission and storage in a small shallow lake. *Hydrobiologia*, *757*(1), 101–115. https://doi.org/10.1007/s10750-015-2240-2

Boehrer, B., & Schultze, M. (2008). Stratification of lakes. *Reviews of Geophysics*, *46*(2), 129–134. https://doi.org/10.1029/2006RG000210

Cai, W.-J., & Wang, Y. (1998). The chemistry, fluxes, and sources of carbon dioxide in the estuarine waters of the Satilla and Altamaha Rivers, Georgia. *Limnology and Oceanography*, *43*(4), 657–668. https://doi.org/10.4319/lo.1998.43.4.0657

Chiu, C.-Y., Jones, J. R., Rusak, J. A., Lin, H.-C., Nakayama, K., Kratz, T. K., et al. (2020). Terrestrial loads of dissolved organic matter drive inter-annual carbon flux in subtropical lakes during times of drought. *Science of The Total Environment*, *717*, 137052. https://doi.org/10.1016/j.scitotenv.2020.137052

Chou, C. H., Chen, T. Y., Liao, C. C., & Peng, C. I. (2000). Long-term ecological research in the Yuanyang Lake forest ecosystem I. Vegetation composition and analysis. *Botanical Bulletin of Academia Sinica*, *41*(1), 61–72.

Christophersen, N., Neal, C., Hooper, R. P., Vogt, R. D., & Andersen, S. (1990). Modelling streamwater chemistry as a mixture of soil-water end-members - A step toward second-generation acidification models. *Journal of Hydrology*, *116*(1), 307–320. https://doi.org/10.1016/0022-1694(90)90130-p

Cole, J. J., & Caraco, N. F. (1998). Atmospheric exchange of carbon dioxide in a low-wind oligotrophic lake measured by the addition of SF6. *Limnology and Oceanography*, *43*(4), 647–656. https://doi.org/10.4319/lo.1998.43.4.0647

Cole, J. J., Prairie, Y. T., Caraco, N. F., McDowell, W. H., Tranvik, L. J., Striegl, R. G., et al. (2007). Plumbing the global carbon cycle: integrating inland waters into the terrestrial carbon budget. *Ecosystems*, *10*(1), 172–185. https://doi.org/10.1007/s10021-006-9013-8

Czikowsky, M. J., MacIntyre, S., Tedford, E. W., Vidal, J., & Miller, S. D. (2018). Effects of wind and buoyancy on carbon dioxide distribution and air-water flux of a stratified temperate lake. *Journal of Geophysical Research: Biogeosciences*, *123*, 2305–2322. https://doi.org/10.1029/2017JG004209

Dalrymple, T. (1960). *Flood-frequency analyses, manual of hydrology: Part 3 (No. 1543-A)*. USGPO.

Downing, J. A., Prairie, Y. T., Cole, J. J., Duarte, C. M., Tranvik, L. J., Striegl, R. G., et al. (2006). The global abundance and size distribution of lakes, ponds, and impoundments. *Limnology and Oceanography*, *51*(5), 2388–2397. https://doi.org/10.4319/lo.2006.51.5.2388

Einsele, G., Yan, J., & Hinderer, M. (2001). Atmospheric carbon burial in modern lake basins and its significance for the global carbon budget. *Global and Planetary Change*, *30*(3–4), 167–195. https://doi.org/10.1016/S0921-8181(01)00105-9

Engel, F., Farrell, K. J., McCullough, I. M., Scordo, F., Denfeld, B. A., Dugan, H. A., et al. (2018). A lake classification concept for a more accurate global estimate of the dissolved inorganic carbon export from terrestrial ecosystems to inland waters. *The Science and Nature*, *105*(3–4), 25. https://doi.org/10.1007/s00114-018-1547-z

Eugster, W., Kling, G., Jonas, T., McFadden, J. P., Wüest, A., MacIntyre, S., & Chapin, F. S., III (2003). CO_2 exchange between air and water in an Arctic Alaskan and midlatitude Swiss Lake: Importance of convective mixing. *Journal of Geophysical Research*, *108*(D12), https://doi.org/10.1029/2002JD002653

GLEON Yuan-Yang Lake site. http://gleon.org/lakes/yuan-yang-lake

Gruber, N., Wehrli, B., & Wüest, A. (2000). The role of biogeochemical cycling for the formation and preservation of varved sediments in Soppensee (Switzerland). *Journal of Paleolimnology*, *24*(3), 277–291. https://doi.org/10.1023/A:1008195604287

Gudasz, C., Bastviken, D., Steger, K., Premke, K., Sobek, S., & Tranvik, L. J. (2010). Temperature-controlled organic carbon mineralization in lake sediments. *Nature*, *466*(7305), 478–481. https://doi.org/10.1038/nature09186

Hooper, R. P., Christophersen, N., & Peters, N. E. (1990). Modelling streamwater chemistry as a mixture of soilwater end-members - An application to the Panola Mountain catchment, Georgia, U.S.A. *Journal of Hydrology*, *116*(1), 321–343. https://doi.org/10.1016/0022-1694(90)90131-G

Hope, D., Palmer, S. M., Billett, M. F., & Dawson, J. J. C. (2004). Variations in dissolved CO_2 and CH_4 in a first-order stream and catchment: An investigation of soil-stream linkages. *Hydrological Processes*, *18*(17), 3255–3275. https://doi.org/10.1002/hyp.5657

Imberger, J. (1985). The diurnal mixed layer 1. *Limnology and Oceanography*, *30*(4), 737–770. https://doi.org/10.4319/lo.1985.30.4.0737

Jähne, B., Münnich, K. O., Bösinger, R., Dutzi, A., Huber, W., & Libner, P. (1987). On the parameters influencing air-water gas exchange. *Journal of Geophysical Research*, *92*, 1937–1949. https://doi.org/10.1029/JC092iC02p01937

Jones, S. E., Kratz, T. K., Chiu, C.-Y., & McMahon, K. D. (2009). Influence of typhoons on annual CO_2 flux from a subtropical, humic lake. *Global Change Biology*, *15*(1), 243–254. https://doi.org/10.1111/j.1365-2486.2008.01723.x

Jones, W. P., & Launder, B. E. (1972). The prediction of laminarization with a two-equation model of turbulence. *International Journal of Heat and Mass Transfer*, *15*, 301–314. https://doi.org/10.1016/0017-9310(72)90076-2

Kimura, N., Liu, W.-C., Chiu, C.-Y., & Kratz, T. (2012). The influences of typhoon-induced mixing in a shallow lake. *Lakes & Reservoirs: Research & Management*, *17*(3), 171–183. https://doi.org/10.1111/j.1440-1770.2012.00509.x

Kimura, N., Liu, W.-C., Chiu, C.-Y., & Kratz, T. K. (2014). Assessing the effects of severe rainstorm-induced mixing on a subtropical, subalpine lake. *Environmental Monitoring and Assessment*, *186*(5), 3091–3114. https://doi.org/10.1007/s10661-013-3603-7

Kimura, N., Liu, W.-C., Tsai, J.-W., Chiu, C.-Y., Kratz, T. K., & Tai, A. (2017). Contribution of extreme meteorological forcing to vertical mixing in a small, shallow subtropical lake. *Journal of Limnology*, *76*(1), 116–128. https://doi.org/10.4081/jlimnol.2016.1477

Kortelainen, P., Rantakari, M., Huttunen, J. T., Mattsson, T., Alm, J., Juutinen, S., et al. (2006). Sediment respiration and lake trophic state are important predictors of large CO_2 evasion from small boreal lakes. *Global Change Biology*, *12*(8), 1554–1567. https://doi.org/10.1111/j.1365-2486.2006.01167.x

Lai, I. L., Chang, S. C., Lin, P. H., Chou, C. H., & Wu, J. T. (2006). Climatic characteristics of the subtropical mountainous cloud forest at the Yuanyang Lake long-term ecological research site, Taiwan. *Taiwania*, *51*(4), 317–329.

Laniak, G. F., Olchin, G., Goodall, J., Voinov, A., Hill, M., Glynn, P., et al. (2013). Integrated environmental modeling: A vision and roadmap for the future. *Environmental Modelling & Software*, *39*, 3–23. https://doi.org/10.1016/j.envsoft.2012.09.006

Lauerwald, R., Laruelle, G. G., Hartmann, J., Ciais, P., & Regnier, P. A. G. (2015). Spatial patterns in CO_2 evasion from the global river network. *Global Biogeochemical Cycles*, *29*, 534–554. https://doi.org/10.1002/2014GB004941

Laurenson, E. M. (1965). Storage routing methods of flood estimation. *Transactions of the Institution of Engineers, Australia. Civil Engineering*, 39–47.

Liu, H., Zhang, Q., Katul, G. G., Cole, J. J., Chapin, F. S., III, & MacIntyre, S. (2016). Large CO_2 effluxes at night and during synoptic weather events significantly contribute to CO 2 emissions from a reservoir. *Environmental Research Letters*, *11*(6), 064001. https://doi.org/10.1088/1748-9326/11/6/064001

Lu, W., Wang, S., Yeager, K. M., Liu, F., Huang, Q., Yang, Y., et al. (2018). Importance of considered organic versus inorganic source of carbon to lakes for calculating net effect on landscape C budgets. *Journal of Geophysical Research: Biogeosciences*, *123*, 1302–1317. https://doi.org/10.1002/2017JG004159

MacIntyre, S. (1993). Vertical mixing in a shallow, eutrophic lake: Possible consequences for the light climate of phytoplankton. *Limnology and Oceanography*, *38*(4), 798–817. https://doi.org/10.4319/lo.1993.38.4.0798

MacIntyre, S., Eugster, W., & Kling, G. W. (2001). The critical importance of buoyancy flux for gas flux across the air-water interface. *Geophysical Monograph-American Geophysical Union*, *127*, 135–139. https://doi.org/10.1029/GM127p0135

MacIntyre, S., Romero, J. R., & Kling, G. W. (2002). Spatial-temporal variability in surface layer deepening and lateral advection in an embayment of Lake Victoria, East Africa. *Limnology and Oceanography*, *47*, 656–671. https://doi.org/10.4319/lo.2002.47.3.0656

Maruya, Y., Nakayama, K., Shintani, T., & Yonemoto, M. (2010). Evaluation of entrainment velocity induced by wind stress in a two-layer system. *Hydrological Research Letters*, *4*, 70–74. https://doi.org/10.3178/hrl.4.70

McDonald, C. P., Stets, E. G., Striegl, R. G., & Butman, D. (2013). Inorganic carbon loading as a primary driver of dissolved carbon dioxide concentrations in the lakes and reservoirs of the contiguous United States. *Global Biogeochemical Cycles*, *27*, 285–295. https://doi.org/10.1002/gbc.20032

Nakamoto, A., Nakayama, K., Shintani, T., Maruya, Y., Komai, K., Ishida, T., & Makiguchi, Y. (2013). Adaptive management in Kushiro Wetland in the context of salt wedge intrusion due to sea level rise. *Hydrological Research Letters*, *7*(1), 1–5. https://doi.org/10.3178/hrl.7.1

Nakayama, K., Komai, K., Tada, K., Lin, H. C., Yajima, H., Yano, S., et al. (2020). Modeling dissolved inorganic carbon considering submerged aquatic vegetation. *Ecological Modelling*, *431*(1), 109188. https://doi.org/10.1016/j.ecolmodel.2020.109188

Nakayama, K., Nguyen, D. H., Shintani, T., & Komai, K. (2016). Reversal of secondary flows in a sharp channel bend. *Coastal Engineering Journal*, *58*(02), 1650002. https://doi.org/10.1142/S0578563416500029

Nakayama, K., Sato, T., Shimizu, K., & Boegman, L. (2019). Classification of internal solitary wave breaking over a slope. *Physical Review Fluids*, *4*(1), 014801. https://doi.org/10.1142/S0578563416500029 10.1103/physrevfluids.4.014801

Nakayama, K., Sato, T., Tani, K., Boegman, L., Fujita, I., & Shintani, T. (2020). Breaking of internal Kelvin waves shoaling on a slope. *Journal of Geophysical Research: Oceans*, *125*, e2020JC016120. https://doi.org/10.1029/2020JC016120

Nakayama, K., Shintani, T., Kokubo, K., Kakinuma, T., Maruya, Y., Komai, K., & Okada, T. (2012). Residual currents over a uniform slope due to breaking of internal waves in a two-layer system. *Journal of Geophysical Research*, *117*, C10002. https://doi.org/10.1029/2012JC008155

Nakayama, K., Shintani, T., Komai, K., Nakagawa, Y., Tsai, J. W., Sasaki, D., et al. (2020). Integration of submerged aquatic vegetation motion within hydrodynamic models. *Water Resources Research*, *56*(8), e2020WR027369. https://doi.org/10.1029/2020wr027369

Nakayama, K., Shintani, T., Shimizu, K., Okada, T., Hinata, H., & Komai, K. (2014). Horizontal and residual circulations driven by wind stress curl in Tokyo Bay. *Journal of Geophysical Research: Oceans*, *119*(3), 1977–1992. https://doi.org/10.1002/2013JC009396

Plummer, L. N., & Busenberg, E. (1982). The solubilities of calcite, aragonite and vaterite in CO_2-H_2O solutions between 0 and 90°C, and an evaluation of the aqueous model for the system $CaCO_3$-CO_2-H_2O. *Geochimica et Cosmochimica Acta*, *46*(6), 1011–1040. https://doi.org/10.1016/0016-7037(82)90056-4

Raymond, P. A., Hartmann, J., Lauerwald, R., Sobek, S., McDonald, C., Hoover, M., et al. (2013). Global carbon dioxide emissions from inland waters. *Nature*, *503*(7476), 355–359. https://doi.org/10.1038/nature12760

Read, J. S., Hamilton, D. P., Desai, A. R., Rose, K. C., MacIntyre, S., Lenters, J. D., et al. (2012). Lake-size dependency of wind shear and convection as controls on gas exchange. *Geophysical Research Letters*, *39*, L09405. https://doi.org/10.1029/2012GL051886

Robertson, D. M., & Imberger, J. (1994). Lake number, a quantitative indicator of mixing used to estimate changes in dissolved oxygen. *International Review of Hydrobiology and Hydrographic*, *79*(2), 159–176. https://doi.org/10.1002/iroh.19940790202

Shade, A., Chiu, C.-Y., & McMahon, K. D. (2010). Seasonal and episodic lake mixing stimulate differential planktonic bacterial dynamics. *Microbial Ecology*, *59*(3), 546–554. https://doi.org/10.1007/s00248-009-9589-6

Smith, S. V. (1985). Physical, chemical and biological characteristics* of CO_2 gas flux across the air-water interface. *Plant, Cell and Environment*, *8*(6), 387–398. https://doi.org/10.1111/j.1365-3040.1985.tb01674.x

Sobek, S., Algesten, G., Bergström, A.-K., Jansson, M., & Tranvik, L. J. (2003). The catchment and climate regulation of pCO_2 in boreal lakes. *Global Change Biology*, *9*(4), 630–641. https://doi.org/10.1046/j.1365-2486.2003.00619.x

Staehr, P. A., & Sand-Jensen, K. (2007). Temporal dynamics and regulation of lake metabolism. *Limnology and Oceanography*, *52*(1), 108–120. https://doi.org/10.4319/lo.2007.52.1.0108

Striegl, R. G., Kortelainen, P., Chanton, J. P., Wickland, K. P., Bugna, G. C., & Rantakari, M. (2001). Carbon dioxide partial pressure and 13C content of north temperate and boreal lakes at spring ice melt. *Limnology and Oceanography*, *46*, 941–945. https://doi.org/10.4319/lo.2001.46.4.0941

Tonetta, D., Staehr, P. A., & Petrucio, M. M. (2017). Changes in CO_2 dynamics related to rainfall and water level variations in a subtropical lake. *Hydrobiologia*, *794*, 109–123. https://doi.org/10.1007/s10750-017-3085-7

Tsai, J.-W., Kratz, T. K., Hanson, P. C., Kimura, N., Liu, W.-C., Lin, F.-P., et al. (2011). Metabolic changes and the resistance and resilience of a subtropical heterotrophic lake to typhoon disturbance. *Canadian Journal of Fisheries and Aquatic Sciences*, *68*(5), 768–780. https://doi.org/10.1139/f2011-024

Tsai, J.-W., Kratz, T. K., Hanson, P. C., Wu, J.-T., Chang, W. Y. B., Arzberger, P. W., et al. (2008). Seasonal dynamics, typhoons and the regulation of lake metabolism in a subtropical humic lake. *Freshwater Biology*, *53*(10), 1929–1941. https://doi.org/10.1111/j.1365-2427.2008.02017.x

Tsai, J.-W., Kratz, T. K., Rusak, J. A., Shih, W.-Y., Liu, W.-C., Tang, S.-L., & Chiu, C.-Y. (2016). Absence of winter and spring monsoon changes water level and rapidly shifts metabolism in a subtropical lake. *Inland Waters*, *6*(3), 436–448. https://doi.org/10.1080/IW-6.3.844

Umlauf, L., & Burchard, H. (2003). A generic length-scale equation for geophysical turbulence models. *Journal of Marine Research*, *61*, 235–265. https://doi.org/10.1357/002224003322005087

Vachon, D., & del Giorgio, P. A. (2014). Whole-lake CO_2 dynamics in response to storm events in two morphologically different lakes. *Ecosystems*, *17*(8), 1338–1353. https://doi.org/10.1007/s10021-014-9799-8

Verpoorter, C., Kutser, T., Seekell, D. A., & Tranvik, L. J. (2014). A global inventory of lakes based on high-resolution satellite imagery. *Geophysical Research Letters*, *41*, 6396–6402. https://doi.org/10.1002/2014GL060641

von Rohden, C., & Ilmberger, J. (2001). Tracer experiment with sulfur hexafluoride to quantify the vertical transport fin a meromictic pit lake. *Aquatic Sciences*, *63*(4), 417–431. https://doi.org/10.1007/s00027-001-8042-9

Wanninkhof, R. (1992). Relationship between wind speed and gas exchange over the ocean. *Journal of Geophysical Research*, *97*(C5), 7373–7382. https://doi.org/10.1029/92JC00188

Weyhenmeyer, G. A., Kosten, S., Wallin, M. B., Tranvik, L. J., Jeppesen, E., & Roland, F. (2015). Significant fraction of CO_2 emissions from boreal lakes derived from hydrologic inorganic carbon inputs. *Nature Geoscience*, *8*(12), 933–936. https://doi.org/10.1038/ngeo2582

Wu, J. T., Chang, S. C., Wang, Y. S., Wang, Y. F., & Hsu, M. K. (2001). Characteristics of the acidic environment of the Yuanyang Lake (Taiwan). *Botanical Bulletin of Academia Sinica*, *42*, 17–22.

Xu, Z., & Xu, Y. J. (2018). Dissolved carbon transport in a river-lake continuum: A case study in a subtropical watershed, USA. *Science of the Total Environment*, *643*, 640–650. https://doi.org/10.1016/j.scitotenv.2018.06.221